Paper:
Sillars, S., Sutcliffe, C., Philo, A., Brown, S., Sienz, J. & Lavery, N. (2017). The three-prong method: a novel assessment of residual stress in laser powder bed fusion. *Virtual and Physical Prototyping*, 1-6.
http://dx.doi.org/10.1080/17452759.2017.1392682

The Three-Prong Method: A Novel Assessment of Residual Stress in Laser Powder Bed Fusion

S.A. Sillars[a,c], C.J Sutcliffe[b,c], A.M. Philo[a,c], S.G.R. Brown[a], J. Sienz[a], N.P. Lavery[a]

Stuart.Sillars@Swansea.ac.uk

[a] *College of Engineering, Swansea University, Bay Campus, Crymlyn Burrows, Swansea, SA1 8EN, UK*

[b] *School of Engineering, University of Liverpool, Brownlow Hill, Liverpool, L69 3GH, UK*

[c] *Renishaw Plc, Additive Manufacturing Products Division, Whitebridge Park, Stone, Staffordshire, ST15 8LQ, UK*

Abstract

Residual stress is a major problem for most metal based Laser Powder Bed Fusion (L-PBF) components. Residual stress can be reduced by appropriate build planning and post-process heat treatments; however, it is not always avoidable and can lead to build failures due to distortion and cracking. Accurate measurement of residual stress levels can be difficult due to high equipment set-up costs and long processing times.

This paper introduces a simple but novel method of measuring residual stresses via a three-pronged cantilever component, the three-prong method (TPM). The method allows for a quick and easy characterisation of residual stress for a wide range of machine parameters, build strategies and materials.

Many different cantilever designs have been used to indicate residual stress within additive manufacturing techniques, such as the ones presented by (Zaeh and Branner, 2010; Yadroitsava *et al.*, 2012, 2015). All of which share the same short-coming, that they indicate stress in one direction. If the principal component of stress is not aligned with the beam geometry it will underestimate peak stress values.

A novel Three-Prong design is proposed which covers 2 dimensions by utilising 3 adjoined cantilever beams, a configuration which echoes that of hole-drilling where three measurements are used to calculate the stress field around a drilled hole. Each arm of the component resembles a curved bridge-like structure; one end of each bridge is cut away from the base plate leaving the centre intact. Deformation of the beams are then measured using a Co-ordinate Measurement Machine. Stress profiles are then estimated using finite element analysis by meshing the deflected structure and forcing it back to its original shape.

In this paper, the new Three-Prong method is used to compare the residual stress levels of components built in Ti-6Al-4V with different hatch patterns, powers and exposure times.

Introduction

Laser Powder Bed Fusion (L-PBF) is an additive layer manufacturing (ALM) technique whereby layers of metal powder are deposited onto a substrate and melted by a focused laser beam. The substrate is lowered and the process is repeated to form a 3D component. This manufacturing technique has allowed designers to create functional, detailed components, quickly and efficiently, leading to cost savings in many areas such as manufacturing tooling for injection moulding and die casting machines, as well as short manufacturing run components. Near net-shape components are created reducing material waste, which in turns allows for the use of more expensive materials such as Ti-6Al-4V. The design process for additive manufacturing is opposite to that of conventional CNC methods, as designers must plan where to add material, instead of planning where to cut away material. This naturally leads to more optimised designs further reducing the amount of raw material used and reducing the weight of the end component. This is especially important in the aeronautical and astronautically industries, where even the most minor weight savings are worth pursuing. Many aerospace companies are already using

ALM to create prototypes components, Stratasys (Hiemenz, no date) reported that NASA used 70 different ALM components on its Mars rovers, but a handful have already committed to using ALM in final production. Up to May, 2017 Thales Alenia space (Alenia, 2017) had reportedly used 79 components created using ALM into space, on their Telkom 3S, SGDC and KOREASAT-7 satellites.

Although ALM has already made its way into final production there are still inherent problems to overcome. In L-PBF laser spot sizes usually have a diameter of between 60-80μm. Meaning that a single layer of a component will be made up of millions of individual spots (in the case of a modulated laser). As the area undergoes thermal expansion when irradiated by the laser beam, the material surrounding it is compressed. The compression causes a part elastic part plastic strain, when the area cools to the surrounding temperature the plastic strain causes a tensile strain in the iradiated zone and a compressive strain in the surrounding area as shown by (Dunbar *et al.*, 2016). The co-efficient of thermal expansion, melting temperature, yield stress, thermal diffusivity of the material and processing parameters such as power and exposure time will control the level of residual stress created by the laser melting process. As the strains caused by the shrinkage achieve higher stress values than the yield stress, the maximum stress will be limited by the yield stress of the material. As the yield strenTherefore the temperature gradients surrounding the melt pool is the greatest influence on residual stress. The chamber is usually heated on most powder-fusion machines but with melt pools with peak temperatures of above 2000°C as shown in the modelling by (Cheng and Chou, 2015) the chamber temperature is a small fraction of this, usually in the range of 100-200°C. Higher chamber temperatures, while having the benefit of reducing residual stress, will cause slower cooling rates, which if high enough can lead to undesirable mechanical properties, such as a reduction in yield strength as shown by (Kempen *et al.*, 2014), (Ali *et al.*, 2017) and (Rafi *et al.*, 2013).

The temperature gradients of the irradiated area and surrounding area are anisotropic due to location on the surface as well as scan strategy. Areas in front and to the sides of the melt pool will be cooler than that behind the melt pool. With hatch strategies being based upon arbitrary starting positions and rotational angles, the principal direction of stress is difficult to predict.

While many components already exist to analyse residual stress they usually take the form of a singular cantilever beam like the ones presented by (Zaeh and Branner, 2010). This configuration can only analyse stress acting lengthways, while the principal component may be misaligned and therefore under-estimated.

Design and Experimental Procedure

The component proposed within this paper comprises of three cantilever beams connected to a central pin. This configuration gives a better indication of stress distribution within the component. Stress throughout the component is anisotropic as temperature gradients around the melt pool will vary due to geometry and scan strategy. Sometimes the melt pool will be surrounded by cold material, while others it could be bordered on 2 sides by recently melted material due to component geometry.

The geometry was re-designed from a pin supported cantilever to an arched bridged design much like the bridge curvature method (BCM) design proposed by (Kruth *et al.*, 2012). This optimises the design for electric discharge machining (EDM) over rotatory saw cutting, speeding up the analysis process. The geometry allows for an automated EDM program to easily cut the supports from the base plate. The deflections are then measured using an automated co-ordinate measuring machine (CMM) program, taking several points at the end of each arm, comparing these deflections to heights measured before cutting.

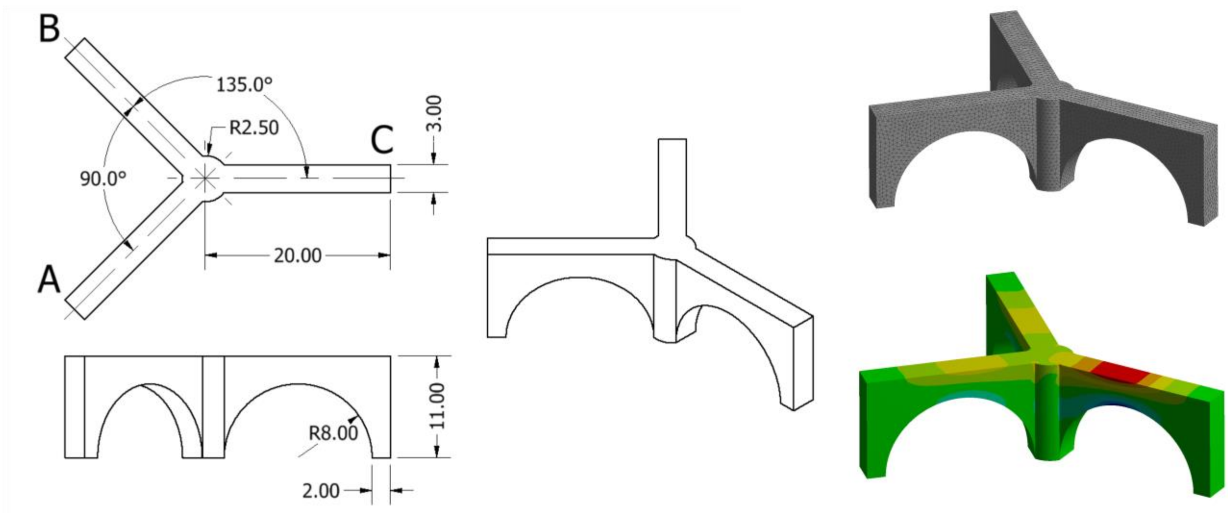

Figure 1 - Three Prong Method Component Dimensions, Mesh and Stress Analysis

Measured deflections are then used in ANSYS to calculate stress profiles. The central pin is fixed while displacements are added to the end of each prong, downwards towards the baseplate. This gives the stress profile apparent in the part before it was cut from the base-plate, an example of this is shown in Figure 1 along with the mesh used.

Ti64 builds were created on a Renishaw RenAM500 using Ti64 powder produced by LPW Technology Ltd. Cheshire, UK with a particle size distribution of 15-48.5µm conforming to ASTM B348 Grade 23 (6%Al, 4%V). The build parameters for 200W build were; 60µm point distance, 70µs exposure time and 95µm hatch spacing. The build parameters for 400W build were; 80µm point distance, 60µs exposure time and 100µm hatch spacing. Both with a layer depth of 60 µm.

Results and Discussion

Initial studies showed that re-scanning the top skin of the component to improve surface finish affected the stress profile. Most CAD slicers will apply a range of parameters to different parts of the component depending on geometry; overhangs, edges and top skins will be given extra passes with the laser or different build parameters all together to improve surface finish and reduce porosity. In this instance, the top skin has been given an extra pass with the laser to induce re-melting, which produces a smoother surface finish. This final pass with the laser travels perpendicular to beam C, causing larger deflections to be seen in beams A and B. Therefore, to mitigate this effect, top skins rescans were turned off for all preceding builds.

As residual stress is built up in the component through thermal expansion, a pore will give the material a void into which it can expand and contract without causing plastic deformation, leading to a reduction in residual stress. This effect has been mitigated by repeating each set of machine parameters across several positions in different areas of the base plate.

Laser Power

Two laser powers are compared in this study, 200W and 400W both using the meander hatch pattern. These laser powers were chosen because suitable build parameters, optimised for highest density already existed. It has been shown by (Tadamalle, Reddy and Ramjee, 2013; Dilip *et al.*, 2016) that laser power has the greatest effect upon weld height, while exposure time has the greatest effect on the weld depth as shown.

The calculated stress results are shown in Figure 2, 400W showed an average mean increase of 5% in calculated max stress when compared to 200W, well within the error bars of the data.

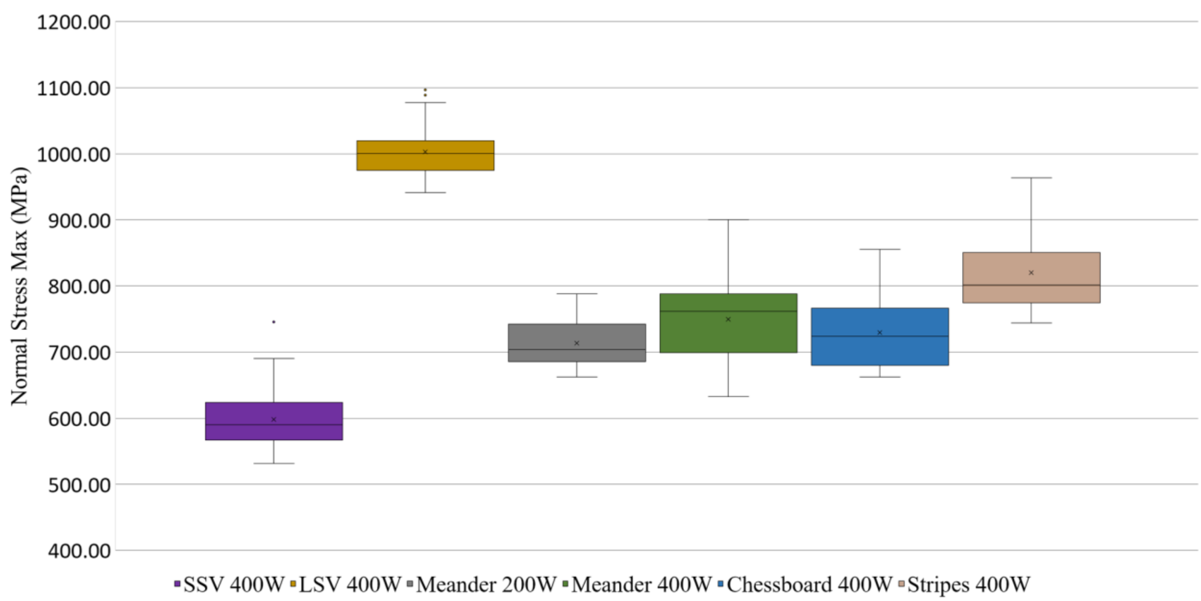

Figure 2 – Calculated Stress Results of TPM Study

Existing Hatch Patterns

Many different scan strategies have been suggested in literature, but the most commonly used scan strategies are meander, chessboard and stripes, therefore these are the ones chosen for this study. Some others of note a fractal and spiral as presented by (Ma and Bin, 2007). Chessboard was created by Concept Laser GmbH to reduce vector length; the chessboard pattern divides the slice into squares of user-defined dimensions. Each square is filled with lines at differing angles, this aims to reduce the number of aligned scan vectors on any given slice. As temperature gradient mechanism (TGM) is assumed to be the driving factor behind residual stress in L-PBF components, the chessboard scan strategy would theoretically decrease the beam deflection by reducing the scan vector lengths as shown by (Mercelis and Kruth, 2006).

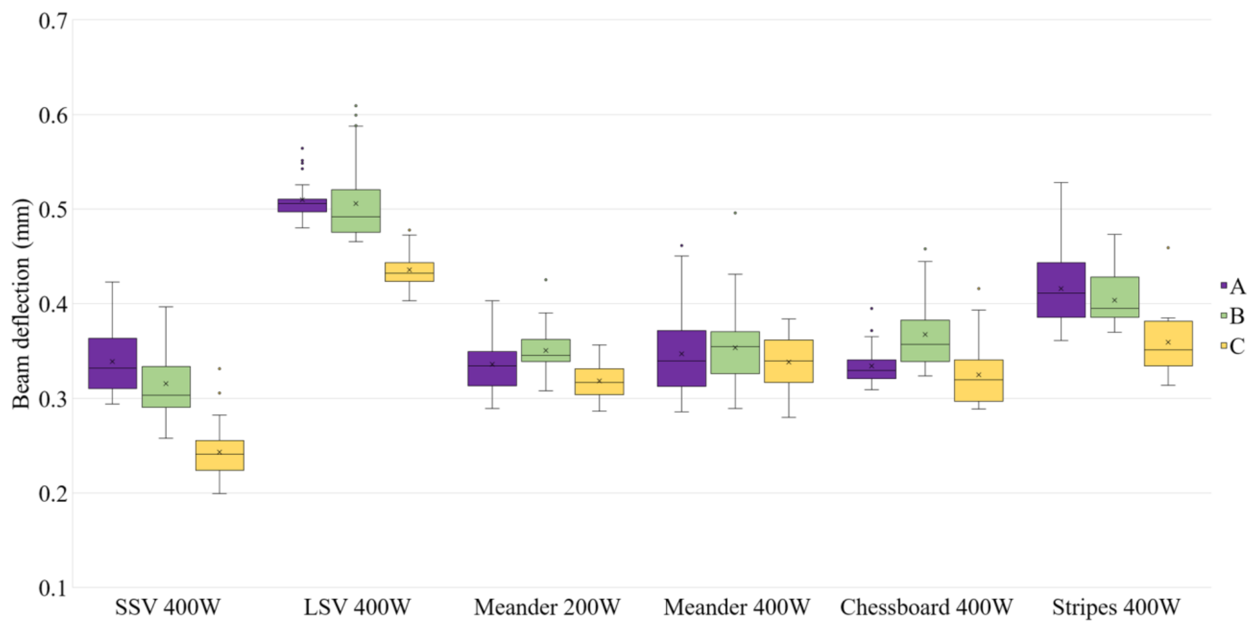

Figure 3 – Beam deflection across beams A, B and C for different scan strategies

However, on any given slice there will be several islands with vectors that align with each other. The longer the geometry is in any given direction, increases the number of scan vectors which will align. In the same way that meander strategy aligns with the longest geometrical spans on some layers, chessboard does partially on every single layer. This shows in the results in Figure 2, meander and chessboard have similar values of peak stress along with stripe scan strategy that is functionally identical to meander.

It can be seen in Figure 3 that meander and chessboard scan strategies give similar values of beam deformation, across all 3 beams, while stripes show the greatest variation.

Long scan vectors

It has been shown by (J.-P. Kruth, E. Yasa, 2009; Kruth *et al.*, 2012) among others (Ina Yadroitsava, 2014; Wu *et al.*, 2014; Dunbar *et al.*, 2016), that longer scan vectors cause higher values of stress aligned with the scan vector when compared to short scan vectors or scan vectors perpendicular to the stress measurement. This has been attributed to the increased temperature of the area of recently irradiated metal behind the melt-pool. As the melt pool will be elongated in the scan direction, the shrinkage in this longitudinal direction will be greatest, while transversal shrinkage will be lesser. It is therefore advantageous to limit the amount of aligned scan vectors within a given layer. A way to achieve this is by aligning the scan vector with the shortest dimension of the current layer. Two scan strategies were tested, a short scan vector (SSV) and a long scan vector (LSV). The three prongs of the TPM component were separated and hatch patterns applied independently, short scan vectors were orientated 90 degrees to the prong, while long scan vectors were applied in line with the prong.

The resulting measured beam deflections can be seen in Figure 3, the short scan vector shows decreased beam deflection when compared to the long scan vector (LSV). While there is a variance in the 3 prongs, possibly due to the 90°-135°-135° angular arrangement, it is obvious that the LSV is the worst-case scenario of scan strategies. Comparing calculated stress values in Figure 2 shows the LSV has ~40% increase in mean stress values over the SSV and a ~25% increase over traditional scan strategies. While the SSV shows a decrease of ~15% over traditional scan strategies. This shows that although these scan strategies have improved on the worst-case scenario they are by no means the complete solution.

Summary

It can be seen from the results shown in Figure 2 that stress in as built components, still attached to the base plate is close to that of the yield strength of the material. In this case the highest calculated stress was in the long scan vector scenario at 1000MPa, with Ti-6Al-4V having a yield strength of 1000-1100 MPa. It is expected that taller wall like structures would achieve even higher values of stress, eventually leading to cracking.

No great difference was found in residual stress levels between the most common scan strategies, however the Short Scan Vector (SSV) showed a ~15% improvement while the Long Scan Vector (LSV) which showed a large increase in beam deflection.

Conclusion

It is clear from the results that improvements to residual stress can be made through smart scan strategies. As hardware improvements become harder and harder to achieve, more emphasis should be put on software. Currently most slicing software takes an STL file and splits them into a series of 2D geometric shapes, then an arbitrary scan strategy is applied. Slicing software should be integrated into CAD software to investigate each slice and apply a scan strategy which considers geometry, possibly guided by a high efficiency multi-scale computational models which can operate in real time. If a slice was split up into a number of squares, with each square being investigated for maximum vector length, the hatch start angle could be set as perpendicular, creating a smart chessboard scan strategy.

Acknowledgements

The authors would like to thank the Additive Manufacturing Products Division at Renishaw Plc., and the Engineering Doctoral Training schemes MATTER (ESPRC funded) and Materials and Manufacturing Academy M2A (European Social Fund). In addition, the authors would like to acknowledge the Centre for Materials Advanced Characterisation (MACH1) for the use of state-of-the-art equipment funded by the Welsh Government and the Advanced Sustainable Manufacturing Technologies (ASTUTE 2020) funded by the Welsh European Funding Office.

References

Alenia, T. (2017) *THALES ALENIA SPACE, THE WORLD CHAMPION IN 3D-PRINTED PARTS IN ORBIT!* Available at: https://www.thalesgroup.com/en/worldwide/space/press-release/thales-alenia-space-world-champion-3d-printed-parts-orbit.

Ali, H. *et al.* (2017) 'In-situ residual stress reduction, martensitic decomposition and mechanical properties enhancement through high temperature powder bed pre-heating of Selective Laser Melted Ti6Al4V', *Materials Science and Engineering A*, 695(February), pp. 211–220. doi: 10.1016/j.msea.2017.04.033.

Cheng, B. and Chou, K. (2015) 'Meltpool Evolution in Selective Laser Melting', in *Solid Freeform Fabrication Symposium*. Austin, Texas, pp. 1182–1194.

Dilip, J. J. S. *et al.* (2016) 'A short study on the fabrication of single track deposits in SLM and characterization', in *Solid Freeform Fabrication Symposium*, pp. 1644–1659.

Dunbar, A. J. *et al.* (2016) 'Development of experimental method for in situ distortion and temperature measurements during the laser powder bed fusion additive manufacturing process', *Additive Manufacturing*, pp. 25–30. doi: 10.1016/j.addma.2016.04.007.

Hiemenz, J. (Stratasys) (no date) *Additive Manufacturing Trends in Aerospace : Leading the Way*. Available at: http://web.stratasys.com/rs/objet/images/SSYS-WP-AeroTrends-03-13-FINAL.pdf.

Ina Yadroitsava, I. Y. C. (2014) 'Evaluation of Residual Stress in Selective Laser Melting of 316L Steel', *Proceedings of the International Conference on Progress in Additive Manufacturing*, (January 2014), pp. 364–369. doi: 10.3850/978-981-09-0446-3.

J.-P. Kruth, E. Yasa, J. D. (2009) 'Experimental investigation of laser surface re-melting for the improvement of selective laser melting process', *14èmes Assises Européennes du Prototypage & Fabrication Rapide, 24-25 Juin*, pp. 1–11. Available at: http://code80.net/afpr/content/assises/2009/actes_aepr2009/papiers/s4_1.pdf.

Kempen, K. *et al.* (2014) 'Selective Laser Melting of Crack-Free High Density M2 High Speed Steel Parts by Baseplate Preheating', *Journal of Manufacturing Science and Engineering*, 136(6), pp. 61026-1-61026–6. doi: 10.1115/1.4028513.

Kruth, J.-P. *et al.* (2012) ‘Assessing and comparing influencing factors of residual stresses in selective laser melting using a novel analysis method’, *Proceedings of the Institution of Mechanical Engineers, Part B: Journal of Engineering Manufacture*, 226(6), pp. 980–991. doi: 10.1177/0954405412437085.

Ma, L. and Bin, H. (2007) ‘Temperature and stress analysis and simulation in fractal scanning-based laser sintering’, *Int J Adv Manuf Technol*, pp. 898–903. doi: 10.1007/s00170-006-0665-5.

Mercelis, P. and Kruth, J.-P. (2006) ‘Residual stresses in selective laser sintering and selective laser melting’, *Rapid Prototyping Journal*, 12, pp. 254–265. doi: 10.1108/13552540610707013.

Rafi, H. K. *et al.* (2013) ‘Microstructures and mechanical properties of Ti6Al4V parts fabricated by selective laser melting and electron beam melting’, *Journal of Materials Engineering and Performance*, 22(12), pp. 3872–3883. doi: 10.1007/s11665-013-0658-0.

Tadamalle, A. ., Reddy, Y. P. and Ramjee, E. (2013) ‘Influence of laser welding process parameters on weld pool geometry and duty cycle’, *Advances in Production Engineering & Management*, 8(1), pp. 52–60.

Wu, A. S. *et al.* (2014) ‘An Experimental Investigation into Additive Manufacturing-Induced Residual Stresses in 316L Stainless Steel’, *Metallurgical and Materials Transactions A: Physical Metallurgy and Materials Science*, 45(13), pp. 6260–6270. doi: 10.1007/s11661-014-2549-x.

Yadroitsava, I. *et al.* (2012) ‘RESIDUAL STRESS IN METAL SPECIMENS PRODUCED BY DIRECT METAL LASER SINTERING’, (2010), pp. 614–625.

Yadroitsava, I. *et al.* (2015) ‘Residual Stress in SLM Ti6Al4V Alloy Specimens’, *Materials Science Forum*, 828–829, pp. 305–310. doi: 10.4028/www.scientific.net/MSF.828-829.305.

Zaeh, M. F. and Branner, G. (2010) ‘Investigations on residual stresses and deformations in selective laser melting’, *Production Engineering*, 4, pp. 35–45. doi: 10.1007/s11740-009-0192-y.